

**A THEORETICAL FRAMEWORK FOR INTERPRETING AND  
QUANTIFYING THE SAMPLING TIME DEPENDENCE OF  
GRAVEL BEDLOAD TRANSPORT RATES**

By

**Kurt Fienberg**

**Arvind Singh**

**Efi Foufoula-Georgiou**

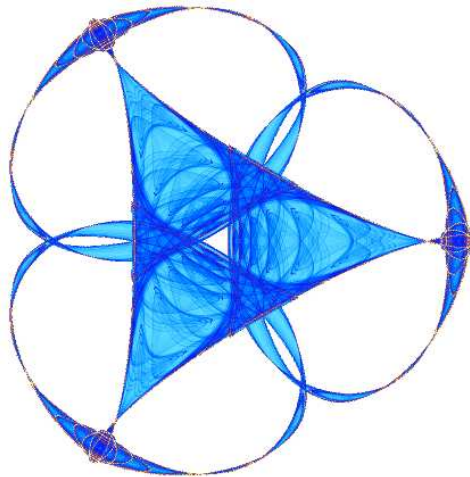
**Doug Jerolmack**

and

**Jeffrey D.G. Marr**

**IMA Preprint Series # 2236**

(February 2009)



**INSTITUTE FOR MATHEMATICS AND ITS APPLICATIONS**

UNIVERSITY OF MINNESOTA  
400 Lind Hall  
207 Church Street S.E.  
Minneapolis, Minnesota 55455-0436

Phone: 612-624-6066 Fax: 612-626-7370

URL: <http://www.ima.umn.edu>

# A Theoretical Framework for Interpreting and Quantifying the Sampling Time Dependence of Gravel Bedload Transport Rates

Kurt Fienberg<sup>1</sup>, Arvind Singh<sup>1</sup>, Efi Foufoula-Georgiou<sup>1</sup>, Doug Jerolmack<sup>1</sup> and Jeffrey D.G. Marr<sup>1</sup>

<sup>1</sup>St. Anthony Falls Laboratory (SAFL) and National Center for Earth-surface Dynamics (NCED)  
University of Minnesota, Minneapolis, MN 55414

## Abstract

Field studies have documented that the average bedload transport rate in gravel bed streams depends on the sampling time (or integration time) over which this average is computed. In this paper we use sediment transport data from a controlled laboratory experiment to document and quantify the dependence on sampling time not only of the mean but of the whole probability density function (pdf) of sediment transport rates in a gravel bed stream. We demonstrate that the higher moments (variance and skewness) scale differently than the mean and we provide a concise parameterization of this statistical scale-dependence. The results indicate that the mean sediment transport rate in moderate flows decreases with increasing sampling time, in agreement with results reported in field studies. The proposed methodology provides a framework within which to seek universal scaling relationships, compare results of different samplers, and also interpret extremes.

## 24 **1. Introduction**

25 In a recent study Bunte and Abt (2005) have provided an excellent account of the problem of  
26 sampling time dependence of gravel bedload transport rate and its importance for interpreting  
27 estimates from different samplers. They also provided a detailed quantification of this dependence  
28 for a range of flows in a gravel-bedded stream. Their results indicated that in moderate to high flows  
29 flows (50% bankfull to almost bankfull conditions) 2 min sampling led to an average transport rate 2  
30 to 5 times lower than that found with 10 min sampling. However, at lower flows (close to the  
31 incipient gravel motion) 2 min sampling overestimated the transport rates at 10 min sampling by a  
32 factor of almost 3. The fact that bedload discharge measurements depend on both sampling time and  
33 mean flow rate was also shown by the field measurements at different time scales documented by  
34 Ergenzinger et al. (1994). In this study we restrict our analysis to the sampling time dependence in  
35 the low flow case, with results from a higher flow experiment to be presented by the authors in a  
36 follow-up work (Singh et al., 2008). The explanation of the sampling interval dependence at low  
37 flow has generally been that the instantaneous sediment transport rates exhibit rare but very high  
38 fluctuations (due to the irregular and stochastic nature of particle movement on the bed) and thus  
39 integrating over variable time intervals changes the chance of sampling these high fluctuations.  
40 Translating this to a statistical interpretation, at very small sampling intervals the chance of sampling  
41 very high fluctuations is small and thus the pdf of sediment transport rates is highly skewed (only a  
42 small number of very high values is present); as the sampling interval increases however, more of  
43 these high fluctuations are likely to be sampled. Although most studies have been concerned only  
44 with how the mean changes with the sampling interval, it is also of interest to study the whole pdf  
45 and quantify how the shape (or the higher order statistical moments) of this pdf change as the scale  
46 (sampling interval) changes. This is important as often it is not only the mean but the variability of

47 the sediment transport rates, including extreme quantiles, that is important in many ecological  
48 studies, e.g., studies that incorporate the effect of bedload sediment on stream habitat.

49 The sampling-time dependence of bedload transport rates has important practical implications  
50 for bedload measurements in the field. Several researchers (e.g. Gomez et al. 1989, Kuhnle 1996,  
51 Wilcock 2001) have argued for sampling durations that are long enough to smooth out fluctuations  
52 and measure the “true mean” transport rate for a particular level of flow. But determining the time  
53 period that fits this criterion requires knowledge of the way in which the statistics of the transport  
54 rate vary with sampling interval. In addition, practical limitations can restrict sampling time to be  
55 less than this ideal: the sampling instrument used may have a limited capacity (such as a Helley-  
56 Smith type sampler), or variations in flow rate may mean that the system can not be considered  
57 stable over such a long period. In such situations, interpreting results and comparing measurements  
58 with different sampling times requires a quantitative understanding of the dependence of bedload  
59 transport on temporal scale.

60 The first objective of this study is to use the results of a controlled and well-instrumented  
61 experimental set-up, described in Section 2, to reproduce some of the effects of sampling interval  
62 that have been observed in the field. By continuously measuring the mass of transported gravel  
63 bedload through an experimental flume at high temporal resolution, and then averaging over  
64 different time intervals, it is possible to simulate sampling the transport rate over different time  
65 periods. The second objective is to develop a theoretical framework for quantifying the variations in  
66 the statistical properties of bedload transport with changing sampling interval. This framework is  
67 outlined in section 3, and is focused on the ideas of scale-invariance, or the search for statistical  
68 quantities that remain the same with change of scale or can be transformed from one scale to another  
69 in a straightforward way. Of course, in this work the scale to which we refer is the temporal scale,

70 i.e. the sampling time of the bedload transport. The results of applying this framework to the  
71 experimental data are presented in section 4, and the implications are discussed in section 5.

## 72 **2. Data Used In This Study**

### 73 **2.1 Experimental set-up and data processing**

74 In order to investigate the dependence of bedload sediment transport on sampling time, we  
75 examine experimental data from the Main Channel facility at the St. Anthony Falls Laboratory,  
76 University of Minnesota. These experiments were conducted as part of a larger-scale experimental  
77 program (called StreamLab06) supported by the National Center for Earth-surface Dynamics  
78 (NCED) at the University of Minnesota. The flume used in this study is 2.74 m wide and 55 m long,  
79 with a maximum depth of 1.8 m. Gravel with a median particle size ( $d_{50}$ ) of 11.3 mm was placed in a  
80 20m long mobile-bed section of the 55 m long channel. The grain size distribution for the bed  
81 material is shown in **Figure 1**. A constant discharge of water at 4300 liters per second was released  
82 into the flume. This was estimated to generate a dimensionless bed stress of about twice the critical  
83 value required to move the bedload sediment (Shields stress = 0.085 using median gravel diameter).  
84 At the downstream end of the test section was located a bedload trap, consisting of 5 weighing pans  
85 of equal size that spanned the width of the channel, as seen in **Figure 2**. Any bedload sediment  
86 transported to the end of the test-section of the channel would fall into the weigh pans, which  
87 automatically recorded the mass they contained every 1.1 seconds. Upon filling with a maximum of  
88 20 kg the weigh pans would tip to release the sediment into the collection hopper located below and  
89 reset the weigh pan.

90 The flume is a partial-recirculating flume; it has the ability to recirculate gravel while water  
91 flows through the flume without recirculation. A large collection hopper located underneath the  
92 weigh pans serves to collect and store gravel dumped out of the weigh drums and also serves as the

93 material source for the recirculation system. The rate of gravel removal out of this hopper and  
94 delivered to the upstream end of the flume via a large pump is set by adjusting the rotation speed of a  
95 large helix, which serves to push gravel laterally out of the hopper and into the recirculation line. In  
96 this way, the collection hopper and helix serve to buffer small fluctuations in sediment flux out of  
97 the flume and provide a more steady “feed-type” delivery of sediment to the upstream end. Because  
98 the physical size of the collection hopper is finite, the auger speed (upstream feed rate) was adjusted  
99 to match the actual transport in the flume such that we would always observe storage of gravel in the  
100 hopper.

101 **FIGURE 1 NEAR HERE**

102 **FIGURE 2 NEAR HERE**

103 Before any measurements were taken, the water supply in the flume was turned on to 4300 liters  
104 per second and was allowed to run 15 hr to develop a dynamic equilibrium in transport and slope  
105 adjustment of the water surface and bed. Determination of the dynamic equilibrium state was made  
106 by checking that the 60 min average flux was stabilized to an almost constant value during the flume  
107 run. The bedload transport data were then recorded continuously for approximately 16 hours through  
108 the rest of the experiment.

109 The raw sediment accumulation data was pre-processed prior to the analysis presented here. The  
110 pre-processing involves removal of weigh pan dumping events from the data and translating the data  
111 set into a continuous accumulation of sediment ( $S_c(t)$ ) time series for each weigh pan over the  
112 duration of the experiment. An example of this series can be seen in Figure 3. A single tipping event  
113 requires the removal of no more than eight data points (~8.8 seconds) of the record. On average, a

114 single weigh pan tipped every 1.5 hr. Overall, the data affected by the weigh pan tipping constitutes  
115 less than 0.15% of the total data record and is, thus, negligible.

116

117 **FIGURE 3 NEAR HERE**

118 The sediment accumulation  $S(t, \Delta t)$  measured over a sampling interval  $\Delta t$  is then simply

119 
$$S(t, \Delta t) = S_c(t + \Delta t) - S_c(t). \quad (1)$$

120 If the sampling interval  $\Delta t$  is taken to be very small, such as the original 1.1 sec resolution of the data  
121 series, one observes a large number of negative values of  $S(t, \Delta t)$ , as shown in **Figure 4a**. These  
122 negative values are clearly not physically plausible since by the experimental design (**Figure 2**) the  
123 sediment can only pass in one direction, down onto the weigh pans, and hence  $S(t, \Delta t)$  should only  
124 be positive. Thus, these negative sediment accumulations are attributed to the mechanical noise  
125 produced by: the natural oscillation of the weigh pans after being hit by the falling gravel; the  
126 fluctuating water surface over the pan; and the vibration caused by the large gravel pump which was  
127 placed near to the weigh pans (for further discussion of the errors associated with weigh pans and  
128 possible processing techniques, see Laronne et al., 2003). This noise can be smoothed out by  
129 considering longer sampling intervals  $\Delta t$ . It was found that the occurrence of negative values of  
130  $S(t, \Delta t)$ , and hence the significance of the noise relative to the signal, was greatly reduced once the  
131 temporal scale  $\Delta t$  was increased to about 2 min. **Figure 4b** shows the time series  $S(t, \Delta t)$  for  $\Delta t = 2$   
132 min. Hence to avoid noise distortion, we will mainly interpret results for temporal aggregation scales  
133 longer than 2 min.

134 **FIGURE 4 NEAR HERE**

135 **2.2 Statistical distribution of the data.**

136 To begin investigating the statistical properties of bedload transport and its dependence on  
137 sampling interval, consider the sediment transport rate, given by  $(S(t, \Delta t) / \Delta t)$ . The pdfs of the  
138 sediment transport rate, calculated at sampling intervals of 2, 5, 10, and 15 min, are shown in **Figure**  
139 **5**. At the smallest scale,  $\Delta t = 2$  min, the probability distribution is wider, with a higher mean and  
140 standard deviation than at the longer sampling intervals. As the sampling interval increases, the  
141 mean decreases slightly and the standard deviation decreases more significantly, as the distributions  
142 become more tightly peaked at longer sampling time. Note that the pdf remains negatively skewed at  
143 the larger temporal scales. One measure of the shape of the probability distribution is the coefficient  
144 of variation,  $C_v$ , which is the ratio of the standard deviation to the mean,  $C_v = \frac{\sigma}{\mu}$ . For the sediment  
145 transport rate,  $C_v$  decreases with increasing temporal scale, as shown in **Figure 6**. So the width of the  
146 pdf, relative to the mean, diminishes with increasing sampling time.

147 **FIGURE 5 NEAR HERE**

148 **FIGURE 6 NEAR HERE**

149 **3. Framework of Analysis**

150 If the sediment transport rate  $(S(t, \Delta t) / \Delta t)$  was independent of the sampling interval, the mean of  
151 the accumulated sediment  $S(t, \Delta t)$  would depend linearly on  $\Delta t$ ; that is, in twice as large a sampling  
152 interval, on the average twice as much sediment would be accumulated,. In practice, however, it has  
153 been found that the mean of  $S(t, \Delta t)$  depends on  $\Delta t$  in a way that has not yet been statistically  
154 characterized. The purpose of this paper is to explore whether this dependence falls under any scale

155 invariance characterization, widely found in turbulence and other geophysical processes (e.g., see  
 156 Parisi and Frisch 1985; Lovejoy et al., 1993; Gupta et al. 1994; Foufoula-Georgiou 1998; Sornette  
 157 and Ouillon 2005; Venugopal et al. 2006, Lashermes and Foufoula-Georgiou, 2007).

158 Let us define the q-th statistical moment  $\langle S(\Delta t)^q \rangle$  as the expectation value of the q-th power of  
 159  $S(t, \Delta t)$ , which is estimated by

$$160 \quad \langle S(\Delta t)^q \rangle = \frac{1}{N} \sum_{t=1}^N (S(t, \Delta t))^q, \quad (2)$$

161 where  $N$  is the total number of data points available at the scale  $\Delta t$ . The 1<sup>st</sup> statistical moment is the  
 162 mean and the 2<sup>nd</sup> statistical moment is a measure of the variability about the origin. Combined, the  
 163 statistical moments  $\langle S(\Delta t)^q \rangle$  for all  $q$  completely capture the shape of the pdf. Statistical scaling, or  
 164 scale invariance, requires that  $\langle S(\Delta t)^q \rangle$  is a power law function of the scale, that is

$$165 \quad \langle S(\Delta t)^q \rangle \propto (\Delta t)^{\tau(q)}, \quad (3)$$

166 where  $\tau(q)$  is the scaling exponent, which is independent of  $\Delta t$  and depends only on the order of the  
 167 moment  $q$ . For a scale-invariant variable, the function  $\tau(q)$  therefore completely determines how the  
 168 pdf of the variable changes with scale. For example, the mean will vary as sampling interval to the  
 169 power of  $\tau(1)$ .

170 The simplest form of scaling, known as simple scaling or monoscaling, is when the scaling  
 171 exponents are a linear function of the moment order i.e. when  $\tau(q) = Hq$ . In this case the single  
 172 parameter  $H$  characterizes how the whole pdf changes over scales, so that if  $P(S(t, \Delta t))$  is the pdf of  
 173 sediment transport at scale  $\Delta t$ , the pdf at a second scale  $\Delta t'$  is given by (e.g., Kumar and Foufoula-  
 174 Georgiou 1993)

$$175 \quad P(S(t, \Delta t')) = \left( \frac{\Delta t}{\Delta t'} \right)^{-H} P \left( \left( \frac{\Delta t}{\Delta t'} \right)^{-H} S(t, \Delta t) \right) \quad (4)$$

176 That is, the pdf at sampling interval  $\Delta t'$  is simply the original pdf normalized by a factor  $\left(\frac{\Delta t}{\Delta t'}\right)^{-H}$ .

177 If  $\tau(q)$  is nonlinear, known as multiscaling, more than one parameter is required to define the  
178 behavior of the probability distribution change over scales. In fact, equation (4) takes on a more  
179 complicated form and involves a convolution of the pdf at the previous scales with a kernel that  
180 depends on the ratio of scales (e.g., Castaing and Dubrulle 1995; see also Venugopal et al. 2006).  
181 Concentrating on the second order moments, one can quantify the relative change in shape of the pdf  
182 with the coefficient of variation,  $C_v$ . Note that  $C_v$  is expressed in terms of the first and second  
183 moments as

$$184 \quad C_v = \left[ \frac{\langle S(\Delta t)^2 \rangle}{\langle S(\Delta t)^1 \rangle^2} - 1 \right]^{1/2}. \quad (5)$$

185 In the presence of scaling (equation 3) this results in

$$186 \quad C_v^2 + 1 \propto (\Delta t)^{\tau(2)-2\tau(1)}, \quad (6)$$

187 which, for the multiscaling case, indicates that the coefficient of variation changes across scales as a  
188 function of  $\tau(2)-2\tau(1)$ . On the contrary, for simple scaling  $\tau(q)$  is linear and hence  $\tau(2) = 2\tau(1)$ , so  
189 that equation (6) means that  $C_v$  will be a constant across scales. The variation in the shape of the pdf  
190 with scale could also be quantified in more detail by higher order dimensionless moments, such as

$$191 \quad \frac{\langle S(\Delta t)^4 \rangle}{\langle S(\Delta t)^2 \rangle^2} \quad (\text{e.g., Mahrt 1988}).$$

## 192 **4. Results**

193 To quantify the scale-dependence of bedload transport, this multiscale analysis methodology was  
194 applied to the experimental sediment transport series described in section 2. The statistical moments  
195  $\langle S(\Delta t)^q \rangle$  are displayed as a function of  $\Delta t$  on a log-log plot in **Figure 7**. If the sediment transport

196 series are scale invariant, we would expect to see a linear relationship in this figure, since the power  
197 law relationship between  $\langle S(\Delta t)^q \rangle$  and  $\Delta t$  expressed in equation (3) is linear on a log-log plot.  
198 Figure 7 indeed shows a linear relationship between the statistical moments and temporal scale over  
199 the range of approximately 1 min to 15 min (indicated by the dashed lines on the figure), and hence  
200 implies a scale invariant regime within this range. At sampling times shorter than 1 min, the  
201 statistical moments do not decrease as would be implied by the scale invariant system, and in fact  
202 increase at short enough scales. This behavior of the statistics at short time-scales is interpreted as  
203 being dominated by the mechanical noise, discussed in section 2.1, which can be identified by the  
204 high frequency of occurrence of negative values in the sediment accumulation rate, which by  
205 experimental design should only be positive. At sampling times  $\Delta t > 15$  min, the statistical moments  
206 also deviate from the log-log linear relationship, eventually leveling out to be relatively constant  
207 with sampling time. This is seen as reaching a critical scale, around 15-30 min, at which the largest  
208 fluctuations of the series are sampled regularly and above which the statistics of the flow are stable.

209 **FIGURE 7 NEAR HERE**

210 **FIGURE 8 NEAR HERE**

211 Within the scaling regime, it can be observed from **Figure 7** that the statistical moments have  
212 different slopes. Estimating these slopes by least squares fitting gives the scaling exponents  $\tau(q)$  for  
213 all moment orders  $q$ , which are plotted in **Figure 8**. Concentrating on first order ( $q = 1$ ) statistical  
214 moment, which is in fact the mean of  $S(t, \Delta t)$ , we see that  $\tau(1) \approx 0.5$ . This implies that within the  
215 scaling range the mean amount of sediment accumulated increases as approximately  $\sqrt{\Delta t}$ , so for  
216 example, if one doubles the sampling interval the amount of mean sediment accumulated does not

217 double but only increases by a factor of about 1.41. When considering the mean sediment transport  
 218 rate,  $(S(t, \Delta t) / \Delta t)$ , this implies that

$$219 \quad \frac{S(t, \Delta t)}{\Delta t} \propto \frac{\sqrt{\Delta t}}{\Delta t} = \Delta t^{-0.5}, \quad (7)$$

220 or that the bedload transport rate decreases with increasing sampling interval  $\Delta t$ . In other words,  
 221 doubling the sampling interval results in a transport rate which is approximately 0.7 ( $=1/\sqrt{2}$ ) times  
 222 smaller.

223 If one then considers the statistical moments of order  $q$  higher than 1, **Figure 8** indicates that  
 224 their scaling exponents  $\tau(q)$  do not increase as a linear power of  $q$  (the theoretical linear relationship  
 225 is shown as a dashed line in the figure for comparison). So  $\tau(2)$  is slightly less than twice  $\tau(1)$ , etc.  
 226 Therefore, the simple scaling described by equation (4) does not hold, and a multiscaling framework  
 227 is required. This is consistent with the fact that we saw in section 2.2 that  $C_v$  decreased with scale,  
 228 corresponding to the pdf narrowing with increasing sampling time: using equation (6), a decreasing  
 229  $C_v$  implies that  $\tau(2)$  is less than  $2\tau(1)$ .

230 Knowledge of the  $\tau(q)$  curve allows the complete rescaling of the pdf with changing sampling  
 231 interval. It is often convenient to parameterize  $\tau(q)$  in order to describe the scaling properties of the  
 232 data in a parsimonious way. Although several nonlinear parameterizations of  $\tau(q)$  are possible, a  
 233 typical parameterization results from assuming that  $\tau(q)$  accepts a polynomial expansion of the form

$$234 \quad \tau(q) = c_0 + c_1 q - \frac{c_2}{2} q^2 + \frac{c_3}{3!} q^3 + \dots, \quad (8)$$

235 with the constants  $c_i$ ,  $i = 0, 1, 2, 3, \dots$  as the model parameters. In this work, due to the uncertainty in  
 236 estimation of higher order moments from limited data, the polynomial is truncated at the second  
 237 order i.e. it is assumed to be quadratic and all  $c_i$  are assumed to be zero for  $i > 2$ . This quadratic  
 238 approximation, which is consistent with the so-called lognormal multiplicative cascade model (e.g.,

239 see Arneodo et al., 1998b), has been found adequate for modeling several geophysical processes  
 240 including atmospheric boundary layer flows (e.g., Basu et al. 2006) and high resolution temporal  
 241 rainfall (Venugopal et al. 2006), among others. The constant  $c_0 = \tau(0)$  is the scaling exponent of the  
 242 zeroth-order moment, which will be equal to zero if the support fills the space, as is the case here.  
 243 This leaves two parameters,  $c_1$  and  $c_2$ , to describe the scaling, which can be obtained by fitting a  
 244 second degree polynomial to the  $\tau(q)$  curve. A least squares fitting was performed on the  
 245 experimental data, and resulted in  $c_1 \approx 0.56$  and  $c_2 \approx 0.05$  (for comparison, for fully developed  
 246 turbulence  $c_1 \approx 1/3$  and  $c_2 \approx 0.025$ ). The  $\tau(q)$  curve fitted with this parameterization is shown as the  
 247 solid curve in **Figure 8**, and can be seen to approximate very well the empirical curve. Assuming  
 248 this model, the mean of the sediment accumulation is seen to scale as  $\langle S(\Delta t) \rangle \propto (\Delta t)^{c_1 - c_2/2}$ , which is  
 249 dominated by the  $c_1$  value, while the scaling of the coefficient of variation is given by  
 250  $(C_v^2 + 1) \propto (\Delta t)^{-c_2}$ . Hence, the parameter  $c_2$  determines the widening of the pdf with decreasing  
 251 scale. Scaling of higher order moments (and the whole pdf) can also be derived in terms of the two  
 252 parameters  $c_1$  and  $c_2$  (e.g., see Venugopal et al., 2006 for an application to rainfall series).

## 253 **5. Discussion and Conclusions**

254 In this study the sampling-time dependence of the statistics of bedload transport has been  
 255 examined, and the statistical moments have been found to change as power law functions of  
 256 sampling time within a range of scales between 1 and 15 min. At temporal scales larger than around  
 257 30 min the statistics were observed to stabilize and become constant with sampling interval. This  
 258 indicates that, at least for this system, the ideal way to measure bedload transport rates, to avoid any  
 259 issues of scale-dependence, would be to use a sampling interval of 30 min or greater. While this  
 260 would certainly be possible in a controlled laboratory experiment such as the one presented here, in  
 261 field studies this approach may not be practical, since we expect that the critical sampling time will

262 scale up with the dimension of the system, and so may require very long sampling times in large  
263 rivers. Such long sampling times may not be feasible if the bedload sampler has a finite capacity or  
264 if the flow conditions in the river change within this time. For this reason further research into the  
265 scale dependence of bedload transport is required, not only to determine the upper limit of variations  
266 with scale, but also to quantify the scale-dependence at shorter sampling times, in order to allow the  
267 correction of statistics in the cases when long sampling times are not feasible.

268 In this work we have outlined a framework to facilitate further investigation into sampling-time  
269 dependence, using the statistical moments of sediment transport to identify regimes of scale-  
270 invariance and scaling exponents  $\tau(q)$  to quantify the changes in the probability distribution with  
271 scale. The quadratic parameterization of  $\tau(q)$ , equation (7), allows description of the continuum of  
272 scaling exponents with just two parameters. This should become increasingly useful in future studies  
273 as experiments are performed in a range of differing conditions and researchers attempt to identify  
274 how the scale-dependence of bedload transport varies with parameters such as flow rate and  
275 sediment size-distribution. In this study, under low flow conditions and with a gravel bed of median  
276 particle size of 11.3mm,  $c_1$  was 0.56 and  $c_2$  was estimated to be 0.05, indicating that the mean  
277 amount of sediment transported increased as approximately the square-root of sampling time. This  
278 means that the sediment transport *rate* decreased as the inverse of the square-root of sampling time  
279 (within the scaling range). However, there is no reason to expect this behavior to be universal for  
280 sediment transport. The flow rate and geometry in this experiment produced a moderate  
281 dimensionless shear stress of approximately twice the critical values for the median grain size.  
282 Preliminary analysis of data from an experiment with a higher flow rate, and hence higher bed-  
283 stress, indicate a reversal of this scaling behavior, with the mean sediment transport rate increasing  
284 with sampling interval through a similar scaling regime. These results will be presented in a further  
285 publication (Singh et al. 2008), along with analysis of the relationship between the modes of

286 sediment transport and the features of the bed elevation, which may explain some of the  
287 characteristic scales of the sediment transport.

288 Another long-term goal for further research is to understand the cause of the observed scaling,  
289 and its connection to the particle-scale dynamics. We believe that the scaling we see is not  
290 completely driven by the near bed turbulence, for the reason that the two-point statistics of the  
291 sediment transport rates (not presented here) do not show long range dependence, which would be  
292 characteristic of the multiplicative mechanism of eddy energy transfer in turbulence (Arneodo et al.  
293 1998a). Instead, there is no long-range correlation, implying a different mechanism giving rise to the  
294 observed scaling, which we suggest might be particle interactions and emergent collective behavior.  
295 Of course, the grain size pdf and the shear stress are both important factors that influence such  
296 particle-scale dynamics and thus would effect the statistics of the resulting sediment transport rates.  
297 Exactly what type of particle-scale dynamics describes the observed statistics remains an open  
298 question which we plan to investigate in the future.

299

## 300 **Acknowledgments**

301  
302 This research was supported by the National Center for Earth-surface Dynamics (NCED), a Science and  
303 Technology Center funded by NSF under agreement EAR-0120914. A series of experiments (known as  
304 StreamLab06) were conducted at the St. Anthony Falls Laboratory as part of an NCED program to  
305 examine physical-biological aspects of sediment transport ([www.nced.umn.edu](http://www.nced.umn.edu)). Computer resources  
306 were provided by the Minnesota Supercomputing Institute, Digital Technology Center at the University  
307 of Minnesota. We would also like to thank the reviewers, Mike Church and Panos Diplas, for their  
308 comments and suggestions.

## 309 **References Cited**

- 310 Arneodo, A., Bacry, E., Manneville, S., and Muzy, J.F., 1998a, Analysis of Random Cascades Using  
311 Space-Scale Correlation Functions, *Phys. Rev. Lett.*, 80, 708 – 711.
- 312 Arneodo, A., Bacry, E., and Muzy, J.F., 1998b, Towards log-normal statistics in high Reynolds number  
313 turbulence, *Eur. Phys. J. B*, 1, 179-209.
- 314 Basu, S., Porté-agel, F., Fofoula-Georgiou, E., Vinuesa, J.F., and. Pahlow, M., 2006, Revisiting the  
315 Local Scaling Hypothesis in Stably Stratified Atmospheric Boundary-Layer Turbulence: an Integration  
316 of Field and Laboratory Measurements with Large-Eddy Simulations, *Boundary-Layer Meteorol.*, 119,  
317 473-500.
- 318 Bunte, K., and Abt, S.R., 2005, Effect of sampling time on measured gravel bedload transport rates in a  
319 coarse-bedded stream, *Water Resources Research*, Vol.41, W11405.
- 320 Castaing, B., and Dubrulle, B., 1995, Fully Developed Turbulence: A Unifying Point of View, *J.*  
321 *Physique II*, 5, 895-899.

322 Ergenzinger, P., de Jong, C., Reid, I., and Laronne, J.B. 1994. Short term temporal variations in bedload  
323 transport rates: Squaw Creek, Montana, USA and Nahal Yatir and Eshtemoa, Israel. p. 251-264 in  
324 Schmidt, C.H. and Ergenzinger, P. (eds.): Lecture Notes in earth Sciences, vol 52: Dynamics and  
325 Geomorphology of Mountain Rivers, Springer Verlag.

326 Foufoula-Georgiou, E., 1998, On scaling theories of space-time rainfall: some recent results and open  
327 problems, In Stochastic Methods in Hydrology: rain, landforms and floods, editors: Barndorff-Nielsen et  
328 al., World Scientific, Singapore.

329 Gomez, B., Naff, R.L., and Hubbell, D.W., 1989, Temporal variations in bedload transport rates  
330 associated with the migration of bedforms, *Earth Surf. Processes Landforms*, 14, 135-156.

331 Gupta, V.K., Mesa, O.J., and Dawdy, D., 1994, Multiscaling theory of floods: Regional quantile  
332 analysis, *Water Resour. Res.*, 30(12), 3405-3421.

333 Kuhnle, R.A., 1996, Unsteady transport of sand and gravel mixtures, in *Advances in Fluvial Dynamics*  
334 and Stratigraphy, eds. P.A. Carling and M. Dawson, John Wiley, Hoboken, N.J., pp 183-201.

335 Kumar, P., and Foufoula-Georgiou, E., 1993, A new look at rainfall fluctuations and scaling properties  
336 of spatial rainfall, *J. Applied Meteorology*, 32 (2), 209-222.

337 Laronne, J.B., Alexandrov, Y., Bergman, N., Cohen, H., Garcia, C., Habersack, H., Powell, M.P. and  
338 Reid, I., 2003. The continuous monitoring of bedload flux in various fluvial environments. p.134-145 in  
339 J. Bogen, T. Fergus and D.E. Walling (eds). *Erosion and Sediment Transport Measurement in Rivers:*  
340 *Technological and Methodological Advances*. Int'l Assoc. Hydrol. Sci. Publ. 283.

341 Lashermes, B., and E. Foufoula-Georgiou, 2007, Area and width functions of river networks: New  
342 results on multifractal properties, *Water Resour. Res.*, 43, W09405, doi:10.1029/2006WR005329.

343 Lovejoy, S., D. Schertzer, P. Silas, Y. Tessier, and D. Lavallée, 1993, The unified scaling model of  
344 atmospheric dynamics and systematic analysis in cloud radiances, *Ann. Geophys.*, 11, 119–127.

345 Mahrt, L., 1988, Intermittency of atmospheric turbulence, *J. Atmos. Sci.*, 46, 79-95.

346 Parisi, G., and Frisch, U., 1985, On the singularity structure of fully developed turbulence, in  
347 Turbulence and Predictability in Geophysical Fluid Dynamics, edited by M. Ghil, R. Benzi and G Parisi,  
348 North -Holland, Amsterdam, 84.

349 Singh, A., K. Fienberg, D. Jerolmack, J. Marr, and E. Foufoula-Georgiou, 2008, Experimental evidence  
350 for statistical scaling and intermittency in sediment transport rates, *under preparation for submission to*  
351 *J. Geophys. Res. (Earth Surface)*.

352 Sornette, D., and G. Ouillon, 2005, Multifractal Scaling of Thermally Activated Rupture Processes,  
353 *Phys. Rev. Lett.*, 94, doi:10.1103/PhysRevLett.94.038501.

354 Venugopal V., Roux, S.G., Foufoula-Georgiou, E., and Arneodo, A., 2006, Revisiting multifractality of  
355 high-resolution temporal rainfall using a wavelet-based formalism, *Water Resources Research*, 42,  
356 W06D14, doi:10.1029/2005WR004489.

357 Wilcock, P.R., 2001, Toward a practical method of estimating sediment transport rates in gravel-bed  
358 rivers, *Earth Surf. Processes Landforms*, 26, 1395-1408.

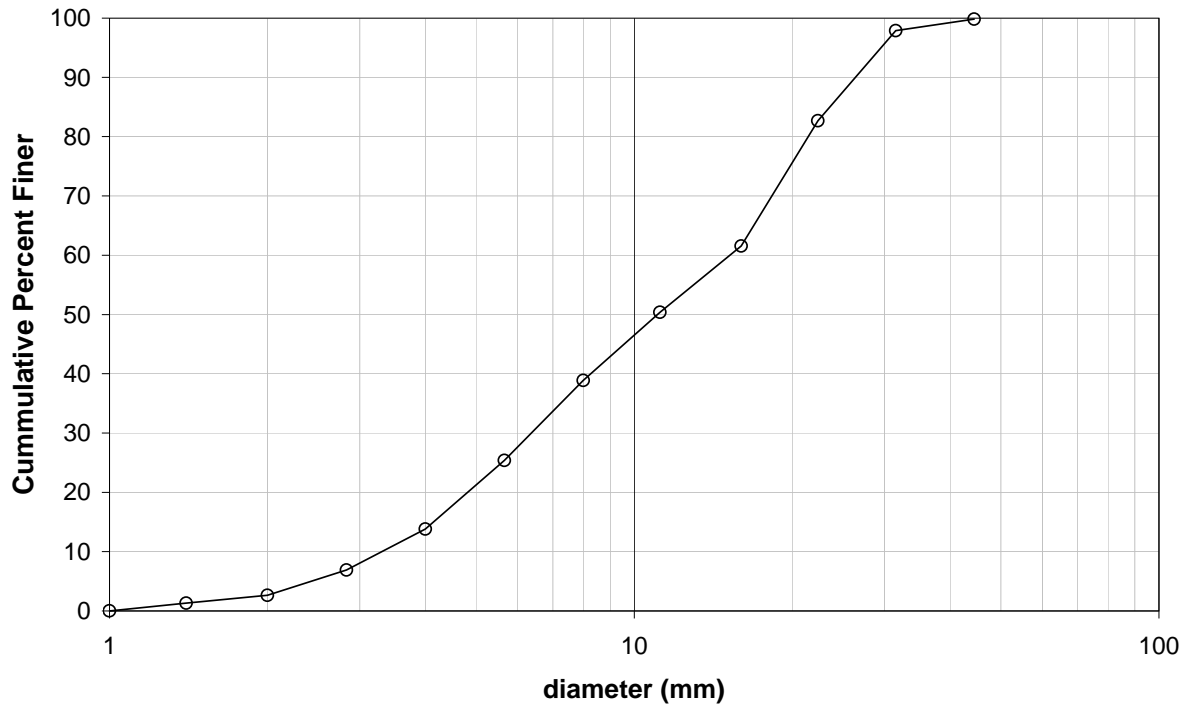


**Figure 1** Grain Size Distribution of the bed surface.



**Figure 2. Weighing Pans located at the downstream end of the test channel. The experiment was conducted at the St. Anthony Falls Laboratory, National Center for Earth-surface Dynamics, University of Minnesota.**

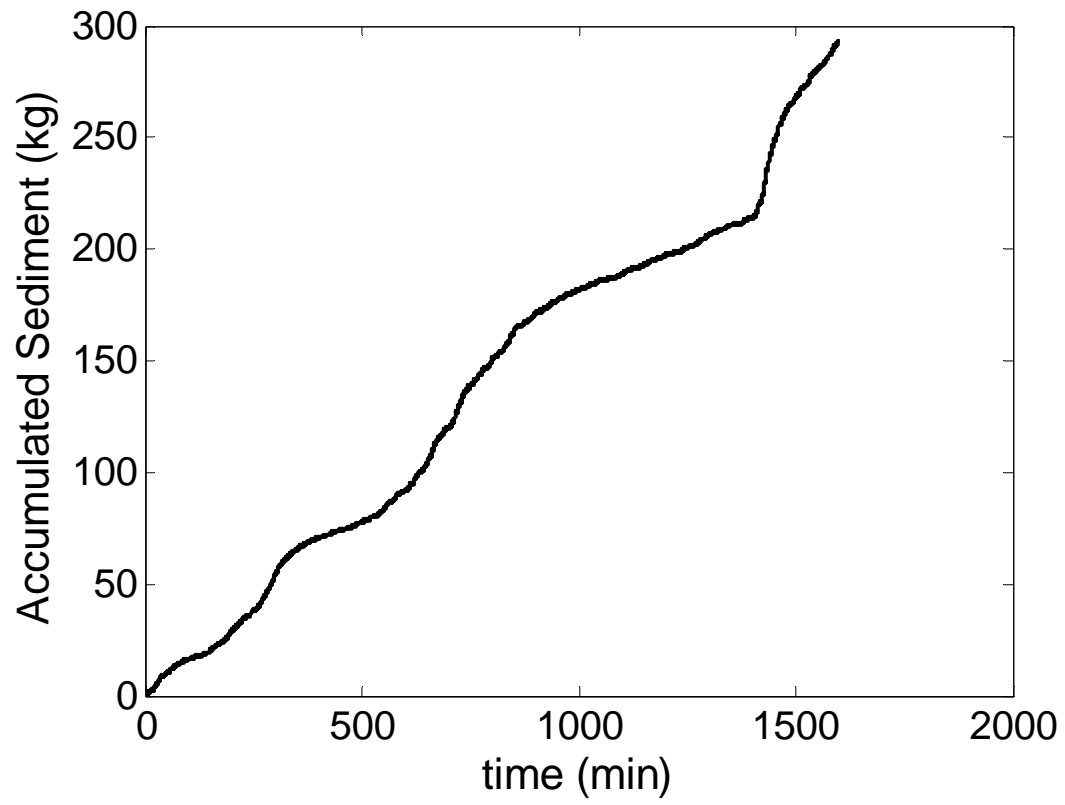


**Figure 3** Time series of the total accumulated sediment  $S_c(t)$

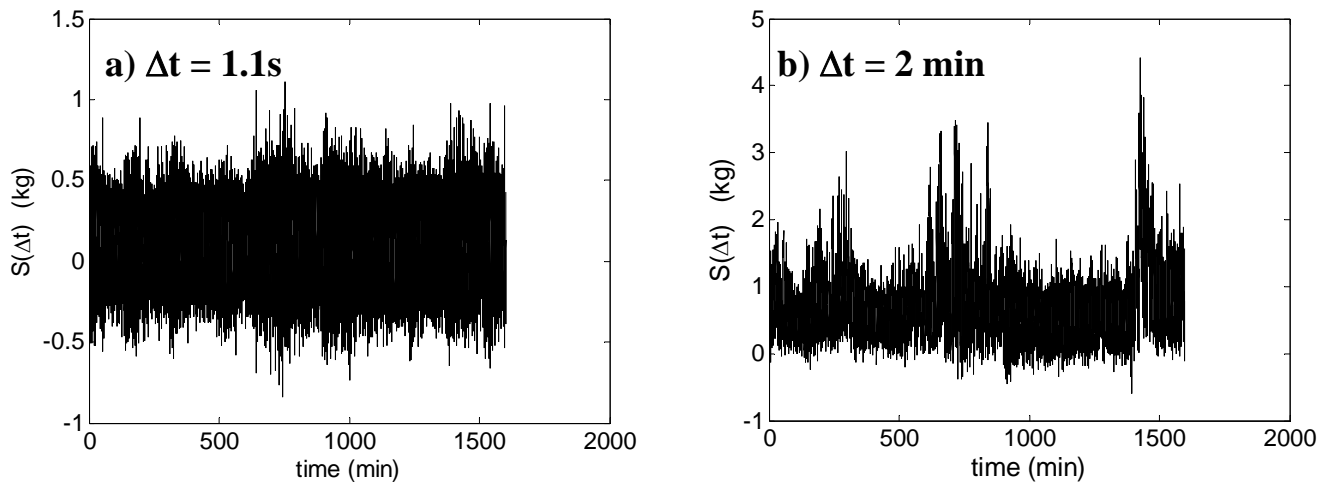


**Figure 4.** The time series of the sediment,  $S(\Delta t)$ , accumulated over sampling intervals  $\Delta t$  of: (a) 1.1 seconds and (b) 2 min

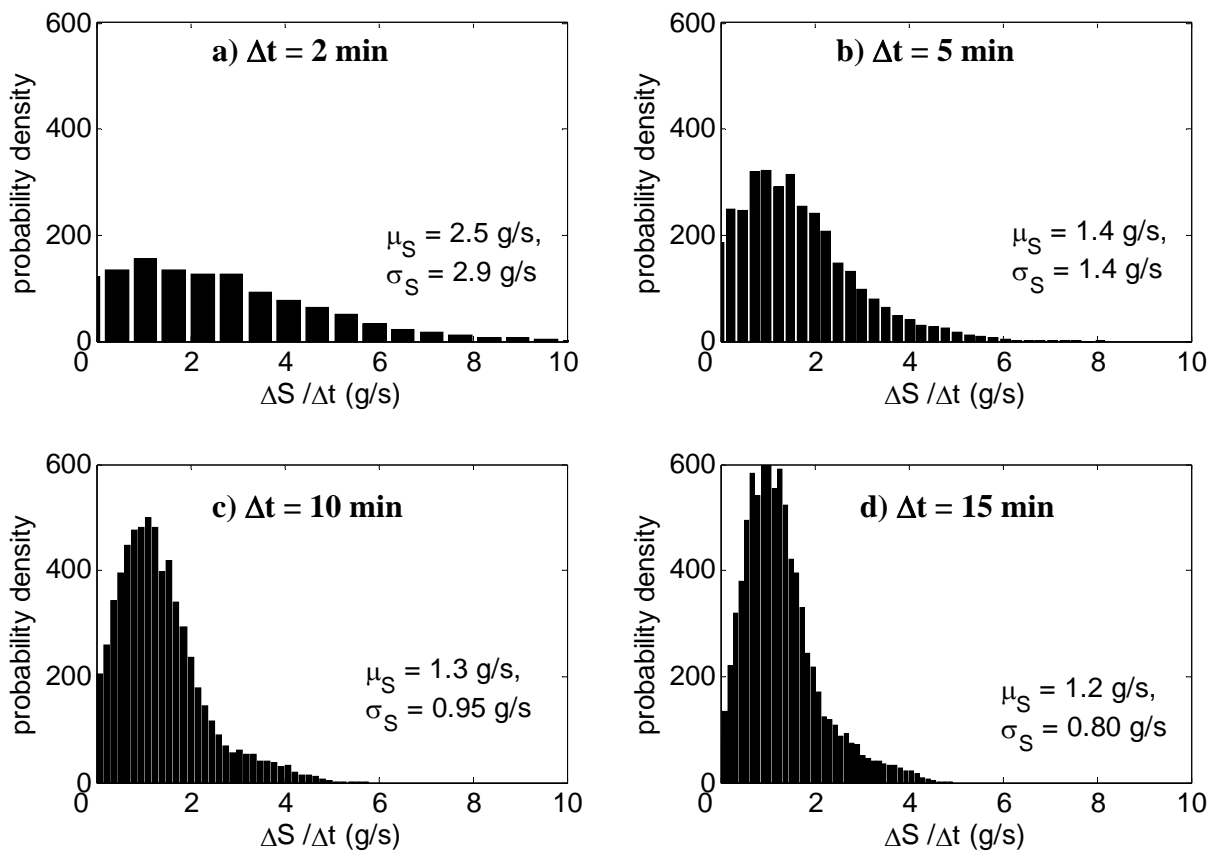


**Figure 5.** Probability density function of sediment transport rate for different sampling intervals (2, 5, 10, 15 min), with mean and standard deviation listed (units of g/s).

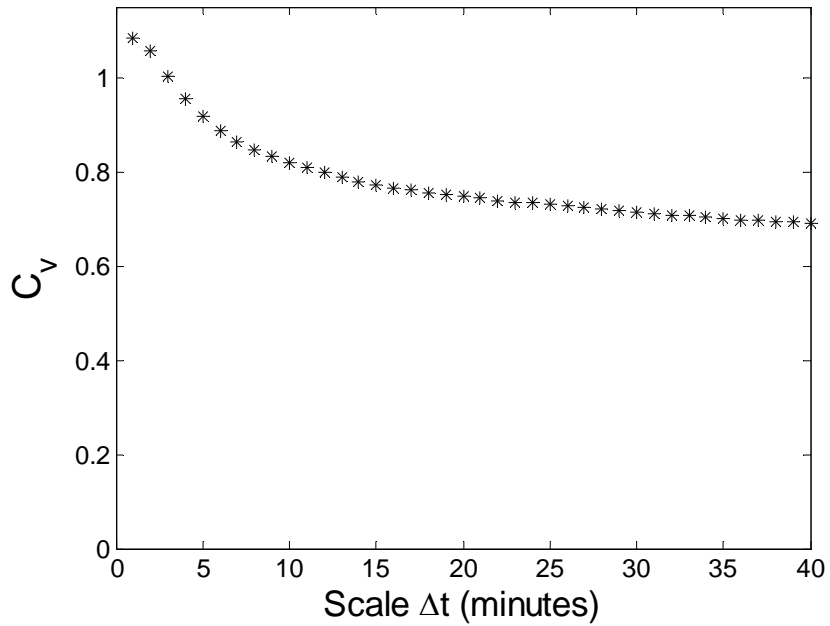


**Figure 6. The coefficient of variation of sediment transport rate as a function of temporal scale  $\Delta t$  (sampling interval).**

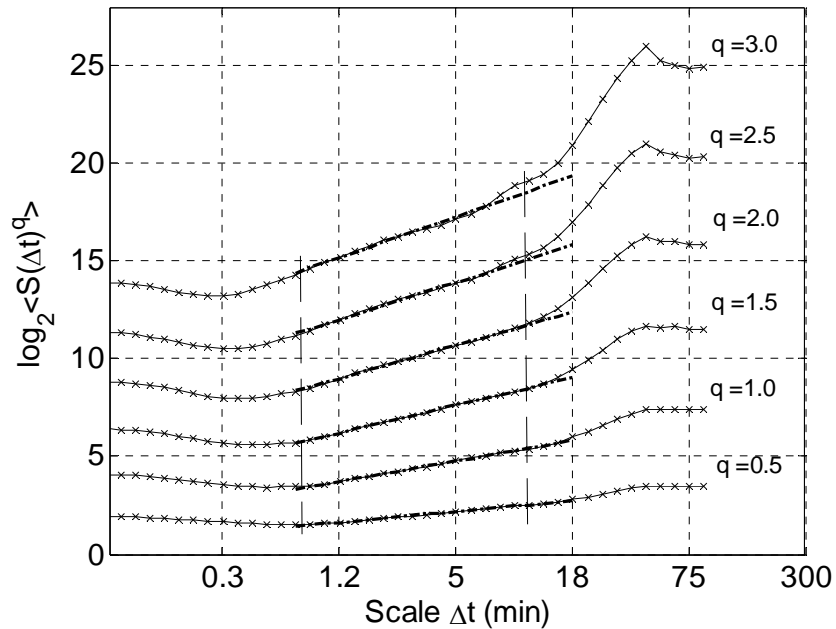


**Figure 7 Statistical moments  $\langle S(\Delta t)^q \rangle$  of the sediment flux as a function of temporal scale (sampling interval), for the range of moment orders  $q = 0.5, 1, 1.5, 2.0, 2.5, 3.0$ . The vertical dashed lines mark the limits of the scaling range.**

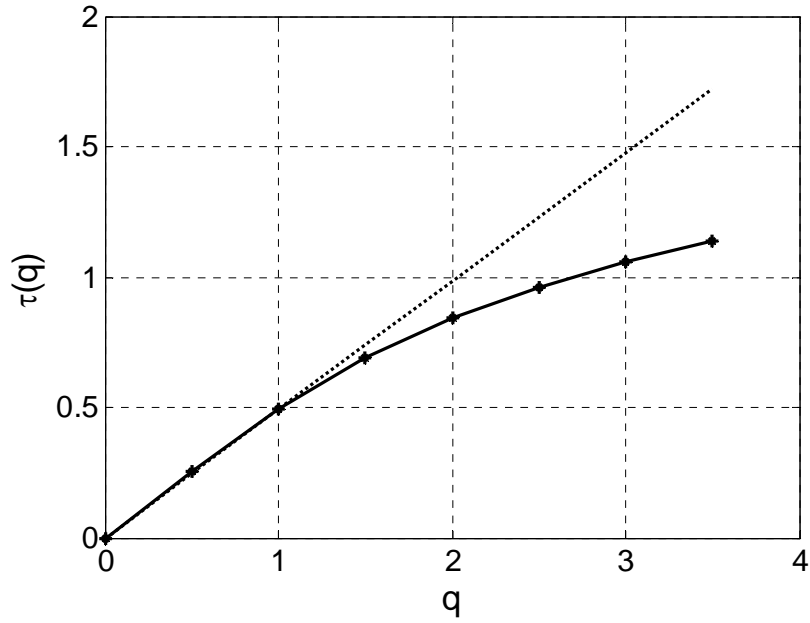


**Figure 8** The scaling exponents  $\tau(q)$  as a function of the moment order  $q$  (computed values from the sediment transport series are shown as points for  $q=0$  to 3 in increments of 0.5 and the solid line is the fitted quadratic approximation). Deviation from monofractality is depicted by the deviation from the straight line.